genes is the target of recurrent translocations in lymphoma (*32*–*34*). Enhancers of the corresponding three gene loci all show a high level of bromodomain containing 4 (BRD4) occupancy in Ly1 cells, a related diffuse large B cell lymphoma cell line, suggesting bromodomain inhibitors such as JQ1 as potential treatments (*35*). Other selectively essential genes included *MEF2B*—a transcriptional activator of *BCL6*—and *CCND3*, both of which are frequently mutated and implicated in the pathogenesis of various lymphomas (*36*). Intriguingly, the top two hits, *CHM* and *RPP25L*, do not appear to have specific roles in B cells; rather, their differential essentiality is likely explained by the lack of expression of their paralogs, *CHML* and *RPP25*, in both of the Burkitt's lymphoma cell lines studied (fig. S6D).

We used two complementary and concordant approaches, CRISPR and gene trap, to define the cell-essential genes in the human genome. Although the gene-trap method is suitable only for loss-of-function screening in rare haploid cell lines, the CRISPR method is broadly applicable. Extending our analysis across different cell lines and tumor types, we developed a framework to assess differential gene essentiality and identify potential drivers of the malignant state. The method can be readily applied to more cell lines per cancer type so as to eliminate idiosyncrasies particular to a given cell line and to more cancer types so as to systematically uncover tumor-specific liabilities that might be exploited for targeted therapies.

REFERENCES AND NOTES

1. G. Giaever *et al.*, *Nature* **418**, 387–391 (2002).
2. L. Cong *et al.*, *Science* **339**, 819–823 (2013).
3. H. Wang *et al.*, *Cell* **153**, 910–918 (2013).
4. T. Wang, J. J. Wei, D. M. Sabatini, E. S. Lander, *Science* **343**, 80–84 (2014).
5. O. Shalem *et al.*, *Science* **343**, 84–87 (2014).
6. H. Koike-Yusa, Y. Li, E. P. Tan, M. C. Velasco-Herrera, K. Yusa, *Nat. Biotechnol.* **32**, 267–273 (2014).
7. J. E. Carette *et al.*, *Science* **326**, 1231–1235 (2009).
8. J. E. Carette *et al.*, *Nature* **477**, 340–343 (2011).
9. I. A. Tchasovnikarova *et al.*, *Science* **348**, 1481–1485 (2015).
10. J. P. Kastenmayer *et al.*, *Genome Res.* **16**, 365–373 (2006).
11. G. S. Cowley, B. A. Weir, W. C. Hahn, *Sci. Data* 10.1038/data.2014.35 (2014).
12. A. C. Wilson, S. S. Carlson, T. J. White, *Annu. Rev. Biochem.* **46**, 573–639 (1977).
13. Y. Ishihama *et al.*, *BMC Genomics* **9**, 102 (2008).
14. H. Jeong, S. P. Mason, A. L. Barabási, Z. N. Oltvai, *Nature* **411**, 41–42 (2001).
15. T. Hart, K. R. Brown, F. Sircoulomb, R. Rottapel, J. Moffat, *Mol. Sys. Biol.* 10.15252/msb.20145216 (2014).
16. Z. Gu *et al.*, *Nature* **421**, 63–66 (2003).
17. H. Liang, W.-H. Li, *Trends Genet.* **23**, 375–378 (2007).
18. B.-Y. Liao, J. Zhang, *Trends Genet.* **23**, 378–381 (2007).
19. T. Makino, K. Hokamp, A. McLysaght, *Trends Genet.* **25**, 152–155 (2009).
20. A. Subramanian *et al.*, *Proc. Natl. Acad. Sci. U.S.A.* **102**, 15545–15550 (2005).
21. Y. Ahmad, F.-M. Boisvert, E. Lundberg, M. Uhlen, A. I. Lamond, *Mol. Cell. Proteomics* **11**, 013680 (2012).
22. J. Barretina *et al.*, *Nature* **483**, 603–607 (2012).
23. A. G. Baltz *et al.*, *Mol. Cell* **46**, 674–690 (2012).
24. T. Sekiguchi, H. Iida, J. Fukumura, T. Nishimoto, *Exp. Cell Res.* **300**, 213–222 (2004).
25. F. L. Muller *et al.*, *Nature* **488**, 337–342 (2012).
26. K. Ohneda, M. Yamamoto, *Acta Haematol.* **108**, 237–245 (2002).
27. L. C. Andersson, K. Nilsson, C. G. Gahmberg, *Int. J. Cancer* **23**, 143–147 (1979).
28. B. S. Andersson *et al.*, *Leukemia* **9**, 2100–2108 (1995).
29. S. Q. Wu *et al.*, *Leukemia* **9**, 858–862 (1995).
30. A. Constantinou, K. Kiguchi, E. Huberman, *Cancer Res.* **50**, 2618–2624 (1990).
31. B. Scappini *et al.*, *Cancer* **100**, 1459–1471 (2004).
32. S. Iida *et al.*, *Blood* **88**, 4110–4117 (1996).
33. H. Bouamar *et al.*, *Blood* **122**, 726–733 (2013).
34. S. Galiègue-Zouitina *et al.*, *C. R. Acad. Sci. III* **318**, 1125–1131 (1995).
35. B. Chapuy *et al.*, *Cancer Cell* **24**, 777–790 (2013).
36. R. D. Morin *et al.*, *Nature* **476**, 298–303 (2011).

ACKNOWLEDGMENTS

We thank T. Mikkelsen for assistance with oligonucleotide synthesis; Z. Tsun for assistance with figures; C. Hartigan, G. Guzman, M. Schenone, and S. Carr for mass spectrometric analysis; and J. Down and J. Chen for reagents for hemoglobin staining. This work was supported by the National Institutes of Health (CA103866) (D.M.S.), the National Human Genome Research Institute (2U54HG003067-10) (E.S.L.), an award from the National Science Foundation (T.W.), and an award from the Massachussetts Institute of Technology Whitaker Health Sciences Fund (T.W.). D.M.S. is an investigator of the Howard Hughes Medical Institute. T.W., D.M.S., and E.S.L. are inventors on a U.S. patent application (PCT/US2014/062558) for functional genomics using the CRISPR-Cas system, and T.W. and D.M.S. are in the process of forming a company using this technology. The sgRNA plasmid library and other plasmids described here have been deposited in Addgene.

SUPPLEMENTARY MATERIALS

www.sciencemag.org/content/350/6264/1096/suppl/DC1
Materials and Methods
Supplementary Text S1 to S5
Figs. S1 to S6
Tables S1 to S6
References (*37*–*50*)

17 October 2014; accepted 1 October 2015
Published online 15 October 2015
10.1126/science.aac7041

GENOME EDITING

Genome-wide inactivation of porcine endogenous retroviruses (PERVs)

Luhan Yang,[1,2,3]*† Marc Güell,[1,2,3]† Dong Niu,[1,4]† Haydy George,[1]† Emal Lesha,[1] Dennis Grishin,[1] John Aach,[1] Ellen Shrock,[1] Weihong Xu,[6] Jürgen Poci,[1] Rebeca Cortazio,[1] Robert A. Wilkinson,[5] Jay A. Fishman,[5] George Church[1,2,3]*

The shortage of organs for transplantation is a major barrier to the treatment of organ failure. Although porcine organs are considered promising, their use has been checked by concerns about the transmission of porcine endogenous retroviruses (PERVs) to humans. Here we describe the eradication of all PERVs in a porcine kidney epithelial cell line (PK15). We first determined the PK15 PERV copy number to be 62. Using CRISPR-Cas9, we disrupted all copies of the PERV *pol* gene and demonstrated a >1000-fold reduction in PERV transmission to human cells, using our engineered cells. Our study shows that CRISPR-Cas9 multiplexability can be as high as 62 and demonstrates the possibility that PERVs can be inactivated for clinical application of porcine-to-human xenotransplantation.

Pig genomes contain from a few to several dozen copies of PERV elements (*1*). Unlike other zoonotic pathogens, PERVs cannot be eliminated by biosecure breeding (*2*). Prior strategies for reducing the risk of PERV transmission to humans have included small interfering RNAs (RNAi), vaccines (*3*–*5*), and PERV elimination using zinc finger nucleases (*6*) or TAL effector nucleases (*7*), but these have had limited success. Here we report the successful use of the CRISPR-Cas9 RNA-guided nuclease system (*8*–*10*) to inactivate all copies of the PERV *pol* gene and effect a 1000-fold reduction of PERV infectivity of human cells.

To design Cas9 guide RNAs (gRNAs) that specifically target PERVs, we analyzed the sequences of publicly available PERVs and other endogenous retroviruses in pigs (methods). Using droplet digital polymerase chain reaction (PCR), we identified a distinct clade of PERV elements (Fig. 1A) and determined that there were 62 copies of PERVs in PK15 cells (a porcine kidney epithelial cell line) (Fig. 1B). We then designed two Cas9 gRNAs that targeted the highly conserved catalytic center (*11*) of the *pol* gene on PERVs (Fig. 1C and fig. S1). The *pol* gene product functions as a reverse transcriptase (RT) and is thus essential for viral replication and infection. We determined that these gRNAs targeted all PERVs but no other endogenous retrovirus or other sequences in the pig genome (methods).

Initial experiments showed inefficient PERV editing when Cas9 and the gRNAs were transiently transfected (fig. S2). Thus, we used a PiggyBac transposon (*12*) system to deliver a doxycycline-inducible Cas9 and the two gRNAs

[1]Department of Genetics, Harvard Medical School, Boston, MA, USA. [2]Wyss Institute for Biologically Inspired Engineering, Harvard University, Cambridge, MA, USA. [3]eGenesis Biosciences, Boston, MA 02115, USA. [4]College of Animal Sciences, Zhejiang University, Hangzhou 310058, China. [5]Transplant Infectious Disease and Compromised Host Program, Massachusetts General Hospital, Boston, MA 02115, USA. [6]Department of Surgery, Massachusetts General Hospital, Harvard Medical School, Boston, MA, USA.
***Corresponding author. E-mail: gchurch@genetics.med.harvard.edu (G.C.); luhan.yang@egenesisbio.com (L.Y.)**
†These authors contributed equally to this work.

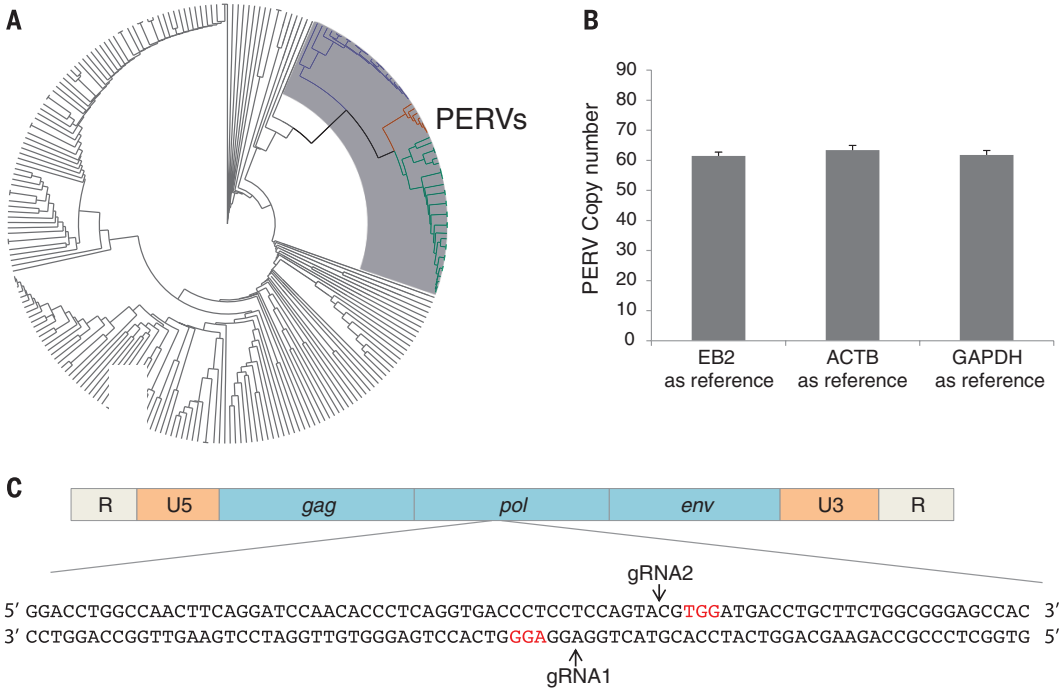

Fig. 1. CRISPR-Cas9 gRNAs were designed to specifically target the *pol* gene in 62 copies of PERVs in PK15 cells. (**A**) Phylogenetic tree representing endogenous retroviruses present in the pig genome. PERVs are highlighted in blue. (**B**) Copy number determination of PERVs in PK15 cells via digital droplet PCR. The copy number of *pol* elements was estimated to be 62, using three independent reference genes: *ACTB*, *GAPDH*, and *EB2*. $n = 3$ independent reference genes, mean ± SEM. (**C**) We designed two CRISPR-Cas9 gRNAs to target the catalytic region of the PERV *pol* gene. The two gRNA targeting sequences are shown below a schematic of PERV gene structure. Their PAM (protospacer adjacent motif) sequences are highlighted in red.

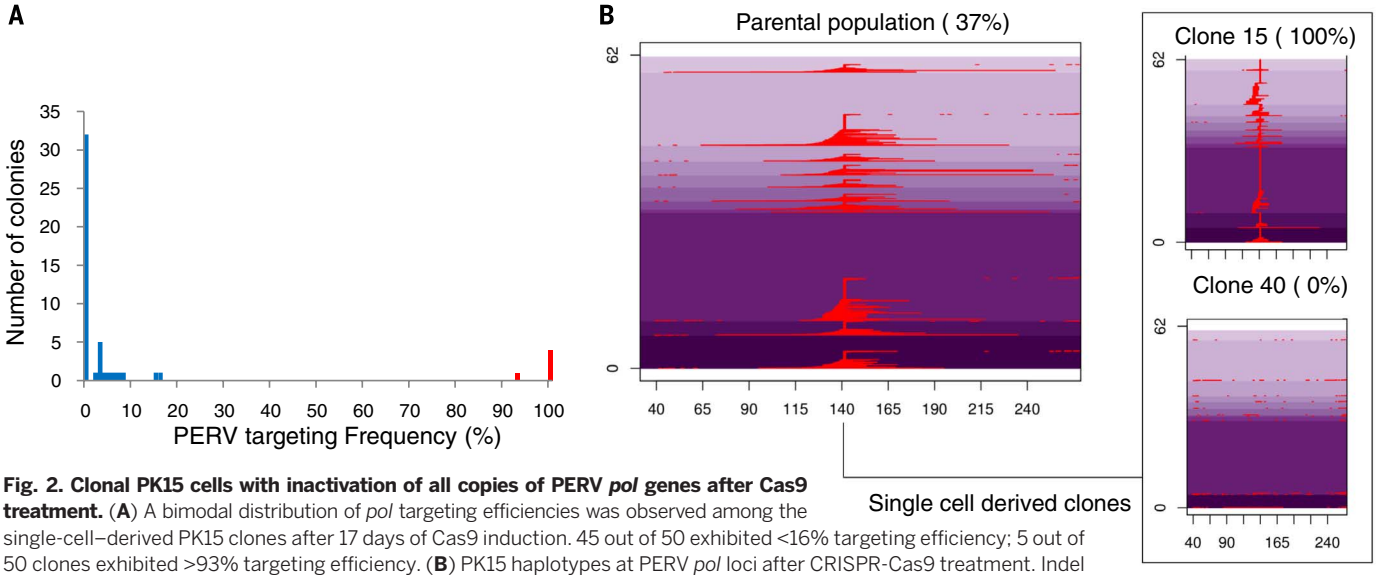

Fig. 2. Clonal PK15 cells with inactivation of all copies of PERV *pol* genes after Cas9 treatment. (**A**) A bimodal distribution of *pol* targeting efficiencies was observed among the single-cell–derived PK15 clones after 17 days of Cas9 induction. 45 out of 50 exhibited <16% targeting efficiency; 5 out of 50 clones exhibited >93% targeting efficiency. (**B**) PK15 haplotypes at PERV *pol* loci after CRISPR-Cas9 treatment. Indel events in the PERV *pol* sequence are represented in red. Shades of purple indicate endogenous PERVs.

into the genome of PK15 cells (figs. S2 and S3). Continuous induction of Cas9 led to increased targeting frequency of the PERVs (fig. S5), with a maximum targeting frequency of 37% (~23 PERV copies per genome) observed on day 17 (fig. S5). Neither higher concentrations of doxycycline nor prolonged incubation increased targeting efficiency (figs. S4 and S5), possibly because of the toxicity of nonspecific DNA damage by CRISPR-Cas9. Similar trends were observed when Cas9 was delivered using lentiviral constructs (fig. S6). We then genotyped the cell lines that exhibited maximal PERV targeting efficiencies. We observed 455 different insertion and deletion (indel) events centered at the two gRNA target sites (Fig. 2B). Indel sizes ranged from 1 to 148 base pairs (bp); 80% of indels were small deletions (<9 bp). We validated the initial deep sequencing results with Sanger Sequencing (fig. S7).

We next sorted single cells from PK15 cells with high PERV targeting efficiency using flow cytometry, and we genotyped the *pol* locus of the resulting clones via deep sequencing (*13*, *14*). A repeatable bimodal (Fig. 2A and figs. S8 and S9) distribution was observed, with ~10% of the clones exhibiting high levels of PERV disruption (97 to 100%) and the remaining clones exhibiting low levels of editing (<10%). We then examined individual indel events in the genomes of these clones (Fig. 2B and figs. S10 and S11). For the highly edited clones (clone 20, 100%; clone 15, 100%; clone 29, 100%; clone 38, 97.37%), we observed only 16 to 20 unique indel patterns in each clone (Fig. 2B and fig. S11). In addition, there was a much higher degree of repetition of indels within each clone than across the clones (fig. S25), suggesting a mechanism of gene conversion in which previously mutated PERV copies were used as templates to repair wild-type PERVs cleaved by Cas9 (Fig. 2B and fig. S25). Mathematical modeling of DNA repair during PERV

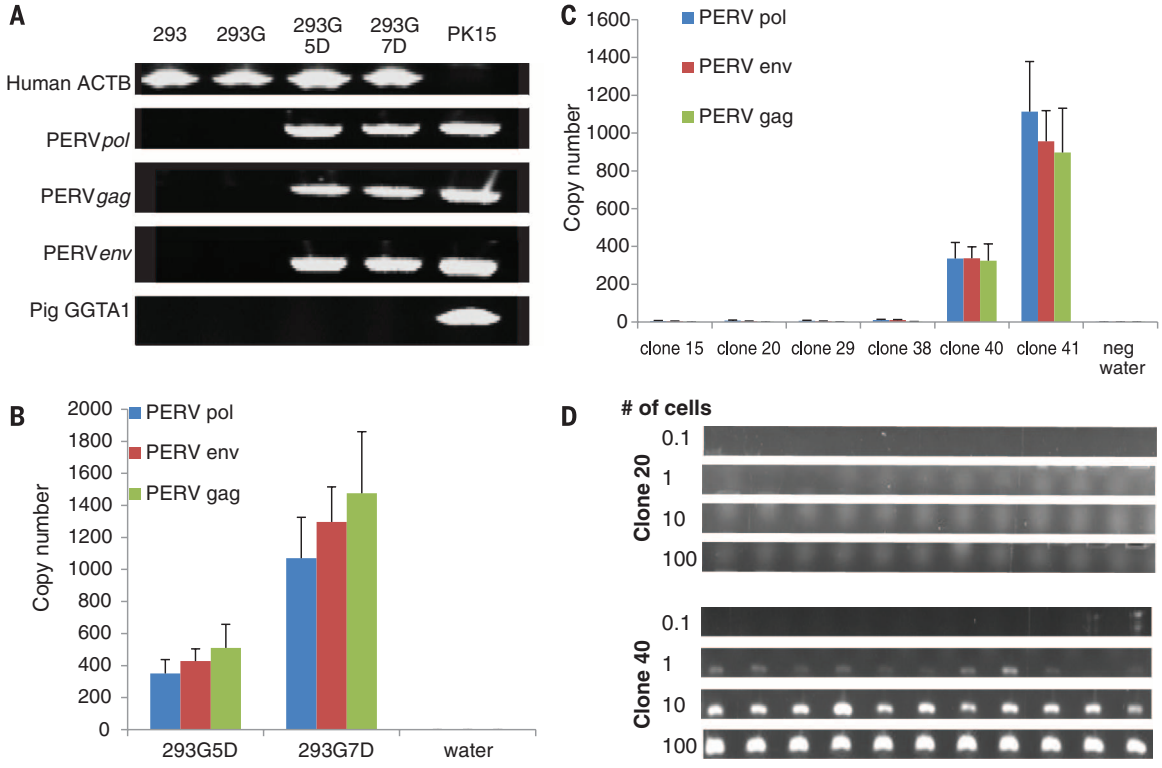

Fig. 3. PK15 cells with all PERV pol genes inactivated lose the infection capacity of human HEK 293 cell lines. (**A**) Detection of PERV *pol*, *gag*, and *env* DNA in the genomes of HEK 293–green fluorescent protein (GFP) cells after coculturing with PK15 cells for 5 and 7 days (293G5D and 393G7D, respectively). A pig GGTA1 primer set was used to detect pig cell contamination of the purified human cells. (**B**) Quantitative PCR (qPCR) analysis of the number of PERV elements in 1000 293G cells derived from a population cocultured with WT PK15 cells using specific primer sets (n = 3 qPCR experiment replicates, mean ± SEM). (**C**) qPCR quantification of the number of PERV elements in PK15 clones 15, 20, 29, and 38, with high levels of PERV *pol* modification and minimally modified clones 40 and 41 (n = 3 qPCR experiment replicates, mean ± SEM). (**D**) Results of PCR on PERV *pol* on genomic DNA from various numbers of HEK 293–GFP cells (0.1, 1, 10, and 100) isolated from populations previously cultured with highly modified PK15 clone 20 and minimally modified clone 40 (see figs. S18 to S21 for a full panel of PCR reactions).

elimination (fig. S26) and analysis of expression data (figs. S22 to S24) supported this hypothesis and suggested that highly edited clones were derived from cells in which Cas9 and the gRNAs were highly expressed.

Next, we examined whether unexpected genomic rearrangements had occurred as a result of the multiplexed genome editing. Karyotyping of individual modified clones (figs. S12 to S14) indicated that there were no observable genomic rearrangements. We also examined 11 independent genomic loci with at most 2 bp mismatches to each of the intended gRNA targets and observed no nonspecific mutations (fig. S27). This suggests that our multiplexed Cas9-based genome engineering strategy did not cause catastrophic genomic instability.

Last, we examined whether our disruption of all copies of PERV *pol* in the pig genome could eliminate in vitro transmission of PERVs from pig to human cells. We could not detect RT activity in the cell culture supernatant of the highly modified PK15 clones (fig. S15), suggesting that modified cells only produced minimal amounts of PERV particles. We then cocultured wild-type (WT) and highly modified PK15 cells with human embryonic kidney (HEK) 293 cells to test directly for transmission of PERV DNA to human cells (*15*). After coculturing PK15 WT and HEK 293 cells for 5 days and 7 days (figs. S16 to S17), we detected PERV *pol*, *gag*, and *env* sequences in the HEK 293 cells (Fig. 3A). We estimated the frequency of PERV infection to be approximately 1000 PERVs per 1000 human cells (Fig. 3B). However, PK15 clones with >97% PERV *pol* targeting exhibited up to 1000-fold reduction of PERV infection, producing results that were similar to background levels (Fig. 3C). We validated these results with PCR amplification of serial dilutions of HEK 293 cells that had a history of contact with PK15 clones (Fig. 3D and figs. S18 to S21). We could consistently detect PERVs in single HEK 293 cells isolated from the population cocultured with minimally modified clone 40, but we could not distinctly detect PERVs in 100 human cells from the population cocultured with highly modified clone 20. Thus, we concluded that the PERV infectivity of the engineered PK15 cells had been reduced by up to 1000-fold.

We successfully targeted the 62 copies of PERV *pol* in PK15 cells and demonstrated greatly reduced in vitro transmission of PERVs to human cells. Although in vivo PERV transmission to humans has not been demonstrated (*18*, *19*), PERVs are still considered risky (*18*, *19*), and our strategy could completely eliminate this liability. Because no porcine embryonic stem cells exist, this system will need to be recapitulated in primary porcine cells and cloned into animals by means of somatic cell nuclear transfer. Moreover, we achieved simultaneous Cas9 targeting of 62 loci in single pig cells without salient genomic rearrangement. To our knowledge, the maximum number of genomic sites previously reported to be simultaneously edited has been six (*20*). Our methods thus open the possibility of editing other repetitive regions of biological significance.

REFERENCES AND NOTES

1. D. Lee *et al.*, *Anim. Biotechnol.* **22**, 175–180 (2011).
2. H.-J. Schuurman, *Xenotransplantation* **16**, 215–222 (2009).
3. J. Ramsoondar *et al.*, *Xenotransplantation* **16**, 164–180 (2009).
4. M. Semaan, D. Kaulitz, B. Petersen, H. Niemann, J. Denner, *Xenotransplantation* **19**, 112–121 (2012).
5. U. Fiebig, O. Stephan, R. Kurth, J. Denner, *Virology* **307**, 406–413 (2003).
6. M. Semaan, D. Ivanusic, J. Denner, *PLOS ONE* **10**, e0122059 (2015).
7. D. Dunn, M. DaCosta, M. Harris, R. Idriss, A. O'Brien, *FASEB J.* **29**, LB761 (2015).
8. M. Jinek *et al.*, *Science* **337**, 816–821 (2012).
9. P. Mali *et al.*, *Science* **339**, 823–826 (2013).
10. L. Cong *et al.*, *Science* **339**, 819–823 (2013).
11. S. G. Sarafianos *et al.*, *J. Mol. Biol.* **385**, 693–713 (2009).
12. M. H. Wilson, C. J. Coates, A. L. George Jr., *Mol. Ther.* **15**, 139–145 (2007).
13. L. Yang *et al.*, *Nucleic Acids Res.* **41**, 9049–9061 (2013).
14. M. Güell, L. Yang, G. M. Church, *Bioinformatics* **30**, 2968–2970 (2014).
15. C. Patience, Y. Takeuchi, R. A. Weiss, *Nat. Med.* **3**, 282–286 (1997).
16. W. Heneine *et al.*, *Lancet* **352**, 695–699 (1998).
17. J. H. Dinsmore, C. Manhart, R. Raineri, D. B. Jacoby, A. Moore, *Transplantation* **70**, 1382–1389 (2000).
18. D. Butler, *Nature* **391**, 320–324 (1998).
19. *ILAR J.* **38**, 49–51 (1997).
20. H. Wang *et al.*, *Cell* **153**, 910–918 (2013).

ACKNOWLEDGMENTS

We thank Z. Herbert and M. Vangala at the Dana-Farber Genomics Core Facility for assistance with RNA analysis, Y. Shen and O. Castanon for volunteering in laboratory research, and S. Broder for scientific advice. M.G. is funded by a Human Frontier Science Program Long Term fellowship. This study was funded by NIH grant P50 HG005550. L.Y., G.C., and M.G. are inventors on a patent filed by Harvard University that covers the work in this manuscript. L.Y., G.C., and M.G. are founding members of eGenesisBio. Pig cells are available from G.C. under a materials transfer agreement with Harvard University.

SUPPLEMENTARY MATERIALS

www.sciencemag.org/content/350/6264/1101/suppl/DC1
Methods
Figs. S1 to S27
References

30 July 2015; accepted 8 October 2015
Published online 15 October 2015
10.1126/science.aad1191

PROTEIN FOLDING

Cotranslational protein folding on the ribosome monitored in real time

Wolf Holtkamp,[1]* Goran Kokic,[1]* Marcus Jäger,[1] Joerg Mittelstaet,[1]† Anton A. Komar,[2] Marina V. Rodnina[1]‡

Protein domains can fold into stable tertiary structures while they are synthesized on the ribosome. We used a high-performance, reconstituted in vitro translation system to investigate the folding of a small five-helix protein domain—the N-terminal domain of *Escherichia coli* N5-glutamine methyltransferase HemK—in real time. Our observations show that cotranslational folding of the protein, which folds autonomously and rapidly in solution, proceeds through a compact, non-native conformation that forms within the peptide tunnel of the ribosome. The compact state rearranges into a native-like structure immediately after the full domain sequence has emerged from the ribosome. Both folding transitions are rate-limited by translation, allowing for quasi-equilibrium sampling of the conformational space restricted by the ribosome. Cotranslational folding may be typical of small, intrinsically rapidly folding protein domains.

In living cells, folding of many proteins begins cotranslationally as soon as the N-terminal part of a given protein emerges from the peptide exit tunnel of the ribosome (*1*–*3*); secondary structure elements, such as α helices, can form within the exit tunnel (*4*–*7*). Whereas small- and medium-size protein domains can acquire their native structures in less than a second (*8*), the bacterial ribosome requires 5 to 10 s to synthesize a protein domain 100 amino acids in length. Cotranslational folding may be attenuated by interactions of the nascent peptide with the ribosome (*9*) and by auxiliary proteins, such as chaperones or other protein biogenesis factors (*10*–*12*). Changes in local translational kinetics, such as those caused by rare codons or transfer RNA (tRNA) abundance, can influence the conformation of newly synthesized proteins (*13*, *14*). Little is known about the exact timing of cotranslational protein folding in relation to protein synthesis or the conformation of the polypeptide emerging from the ribosome.

To monitor cotranslational protein folding during ongoing translation, we used a reconstituted in vitro translation system in combination with the selective site-specific labeling of nascent proteins with fluorescent probes (*15*). We studied the N-terminal domain (NTD) of *Escherichia coli* N5-glutamine methyltransferase HemK. The HemK NTD consists of five helices (residues 3 to 12, 20 to 29, 35 to 42, 48 to 65, and 67 to 73) (Fig. 1) connected by a linker (residues 72 to 96) to the C-terminal domain (CTD) (*16*). The isolated HemK NTD (residues 1 to 73) forms a stable α-helical structure independent of the CTD (figs. S1 and S2). Free NTD in solution folds on a (sub)millisecond time scale in a predominantly two-state fashion (fig. S3 and table S1). For in vitro translation, we used an mRNA construct coding for the N-terminal 112 amino acids of HemK (HemK112) comprising the NTD (73 amino acids) plus 39 amino acids from the linker and the CTD. This length should allow the NTD to fully emerge from the ribosome exit tunnel when HemK112 is synthesized (Fig. 1).

We rapidly mixed synchronized initiation complexes containing BodipyFL (BOF)–Met-tRNA^{fMet} with elongation factors (EF-Tu, EF-Ts, and EF-G) and purified aminoacyl-tRNAs. Instead of Lys-tRNA, we added εNH$_2$-Bodipy576/589 (BOP)–Lys-tRNA^{Lys} to introduce the second fluorescence label at position 34 of the nascent peptide (Fig. 1). The two reporters provide a donor-acceptor pair to monitor Förster resonance energy transfer (FRET). Donor- and acceptor-only controls served to correct the time courses measured in the presence of both donor and acceptor (fig. S4A). The appearance of FRET after 10 s (Fig. 2A and fig. S4C) implies the formation of a structure in which positions 1 and 34 of HemK112 come into close proximity to one another. When compared to the time course of translation, the band representing the full-length protein appears after 40 s (Fig. 2B and fig. S5). Thus, chain compaction begins earlier than the full-length domain emerges from the ribosome.

We translated HemK peptides of different lengths ranging from 42 to 112 residues (Figs. 1A and 2B) and derived a translation velocity of 3.6 ± 0.1 amino acids/s (Fig. 2B and fig. S5B). Translation of HemK42 results in a low final FRET efficiency, reflecting an extended conformation of short nascent chains within the exit tunnel (Fig. 2, B and C). Synthesis of HemK56 leads to the formation of a high-FRET state, which suggests that the two probes come close—presumably by compaction of the nascent peptide—even though BOP-Lys on the nascent HemK56 chain should be occluded inside the tunnel, even when the peptide is in a fully extended conformation (Fig. 1A). Thus, the structure manifested by high FRET must form largely inside the ribosome, close to the exit of the peptide tunnel. With the HemK70 construct, the FRET efficiency is even higher, and the time of FRET appearance coincides with the synthesis of the 70–amino acid product (Fig. 2B). For all constructs, FRET rapidly increases after ~10 s of translation, whereas the formation of full-length HemK84, 98, and 112 is markedly slower than the appearance of the high-FRET state.

The final FRET efficiency is somewhat lower for HemK84, 98, and 112 relative to HemK70, indicating that there are structural rearrangements when the peptide chain becomes longer than 70 amino acids (Fig. 2C). With fully translated HemK112, the entire 73–amino acid NTD is likely to emerge from the exit tunnel, and thus the lower FRET level reflects the end state of folding. In contrast, the conformation captured by using the HemK70 construct does not represent a native-like fold, but rather a compact state that is stabilized by the ribosome until the next part of the protein sequence emerges. When we released the nascent HemK70 peptide from the ribosome by puromycin treatment, the FRET efficiency decreased to the level measured with the longer constructs (Fig. 2C and fig. S6), reflecting spontaneous domain folding (fig. S3). The decrease of FRET in HemK112 is attributable to the stabilization of the N terminus: BOP-Lys^{34} is in close proximity to Tyr^{3}, which can quench BOP fluorescence (*17*, *18*). When we substituted Tyr^{3} with Phe, we recovered the high FRET signal (Fig. 2C). These data indicate the existence of two states along the folding pathway of the NTD: a compact state, formed early during translation, which rearranges into a near-native fold upon further translation.

We probed the folding of HemK nascent peptides of different lengths by limited proteolysis with thermolysin, which cleaves at sites with bulky and aromatic residues (*19*), and monitored the

[1]Department of Physical Biochemistry, Max Planck Institute for Biophysical Chemistry, 37077 Göttingen, Germany. [2]Center for Gene Regulation in Health and Disease and Department of Biological, Geological and Environmental Sciences, Cleveland State University, Cleveland, OH 44115, USA.
*These authors contributed equally to this work. †Present address: Miltenyi Biotec GmbH, 51429 Bergisch Gladbach, Germany.
‡Corresponding author. E-mail: rodnina@mpibpc.mpg.de

Science

Genome-wide inactivation of porcine endogenous retroviruses (PERVs)

Luhan Yang, Marc Güell, Dong Niu, Haydy George, Emal Lesha, Dennis Grishin, John Aach, Ellen Shrock, Weihong Xu, Jürgen Poci, Rebeca Cortazio, Robert A. Wilkinson, Jay A. Fishman and George Church

Science **350** (6264), 1101-1104.
DOI: 10.1126/science.aad1191originally published online October 11, 2015

Virally cleansing the pig genome

Transplants from pigs could be a solution to a shortage of human organs for transplantation. Unfortunately, porcine endogenous retroviruses (PERVs) are rife in pigs and can be transmitted to humans, risking disease. L. Yang *et al.* integrated CRISPR-Cas into the pig cell genome, where continuous induction of the Cas9 editing enzyme resulted in the mutation of every single PERV reverse transcriptase gene. This prevented replication of all copies of PERV, viral infection, and transmission to human cells.

Science, this issue p. 1101

Science (print ISSN 0036-8075; online ISSN 1095-9203) is published by the American Association for the Advancement of Science, 1200 New York Avenue NW, Washington, DC 20005. The title *Science* is a registered trademark of AAAS.